Electronic supplementary information

Fluorinated carbon fiber as a novel nanocarrier for cancer chemo-photothermal therapy

Lu Sun, Peiwei Gong*, Xicheng Liu, Minghui Pang, Meng Tian, Jinyu Chen, Jiuyao Du, Zhe Liu*

Institute of Anticancer Agents Development and Theranostic Application, The Key Laboratory of Life-Organic Analysis and Key Laboratory of Pharmaceutical Intermediates and Analysis of Natural Medicine, Department of Chemistry and Chemical Engineering, Qufu Normal University, Qufu 273165, P. R. China

1. FTIR spectra of HFC at different designed ratio

On the basis of previous work about the phase equilibria of KOH and NaOH, when the weight ratio of NaOH is 43.1% the eutectic point of the mixture of NaOH and KOH at around 170 ^{o}C and the lowest freezing point at about 174.5 ^{o}C. In view of the fact that oxygen groups on FC could fast decompose when the temperature more than 200 ^{o}C, then 180 ^{o}C was setted as the reaction temperature meanwhile the weight ratio of NaOH is 43.1% of the mixed alkali.

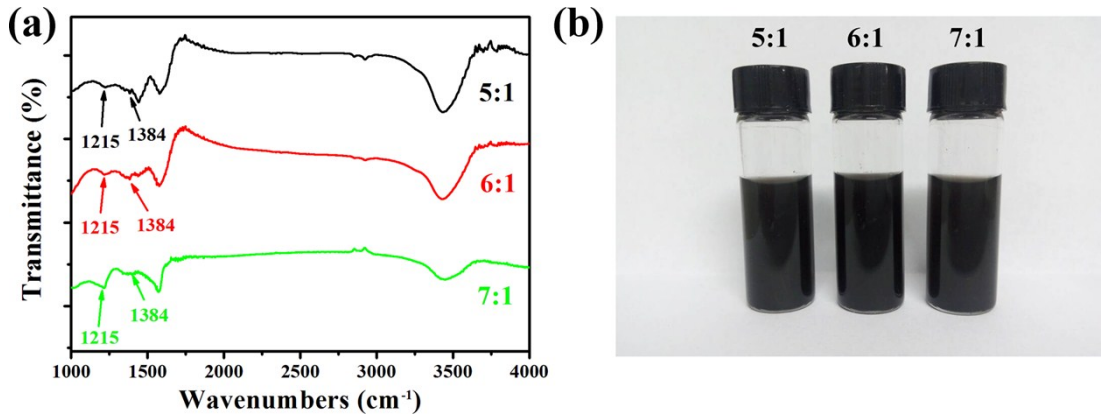

Fig. S1. Chemical composition analysis (a) FTIR spectra of HFC at different designed ratio. (b) The digital images of HFC dispersed in water.

According to the previous exploration experiment, the weight ratio of alkali/FC at 5, 6 and 7 were selected to synthesize HFC, and meanwhile the high fluoride content was maintained. Fig. S1 (a) showed FTIR spectra of HFC at three designed ratio, which clearly indicated that besides covalent C–F bond (1215 cm^{-1}), C–O bond in the form of C–OH (1384 cm^{-1}) also can be found on the structure of HFC. It was worth noting that the three designed ratio displayed the same results of HFC, then the weight ratio of alkali/FC at 5 was selected. HFC showed finer hydrophilicity and dispersibility after mixed alkali treatmen, the digital images of HFC for three designed ratio dispersed in water (Fig. S1 (b)).

2. UV–vis absorption spectra of HFC and FCO

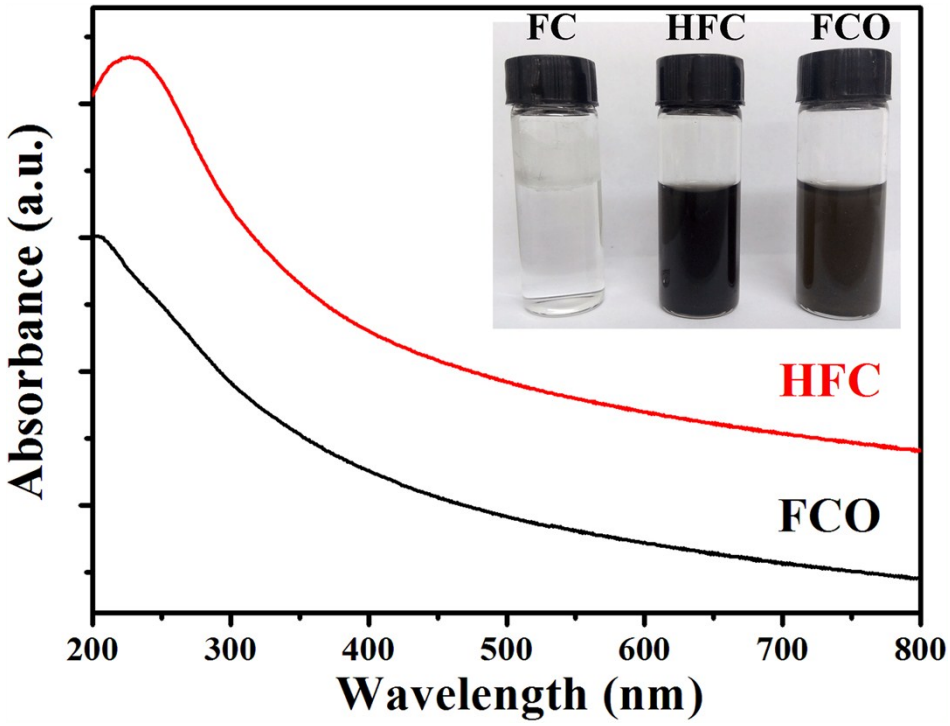

Fig. S2. UV–vis absorption spectra of HFC and FCO (the inset shows the digital image of FC, HFC and FCO dispersed in water).

Fig. S2 showed UV–vis absorption spectra of HFC and FCO, which with excellent hydrophilicity and dispersibility and the inset showed the digital image of FC, HFC and FCO dispersed in water.

3. The size distribution histogram of FCO and DLS of the size distribution of FCO

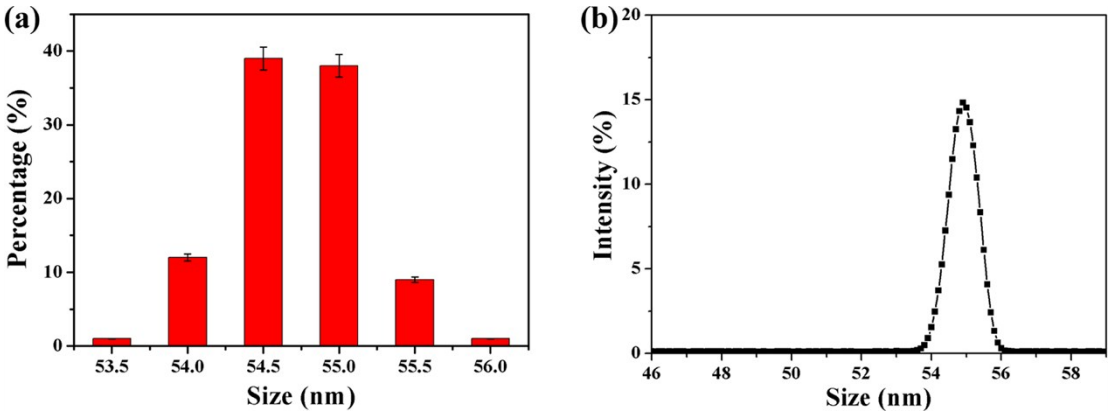

Fig. S3 (a) The size distribution histogram of FCO. (b) The DLS data of FCO.

4. Calculation of the photothermal conversion efficiency (η)

There are many methods to calculate the photothermal conversion efficiency (η) of photothermal materials[1-5]. In this work, in order to assess η, FCO was continuously irradiated with 1.8 W/cm^2 laser until the solution reached a steady-state temperature, and the variation of the temperature was recorded as a function of time. Subsequently, closed the laser and the temperature of aqueous solution decreased, then the rate of heat transfer from the dispersion system to environment was measured. The η value was calculated using the following eqn (1) and eqn (2):

$$\eta = \frac{hS(T_{max} - T_{surr})}{I(1-10^{-A_{808}})} (1)$$

$$\tau_s = \frac{m_{H_2O} C_{H_2O}}{hS} (2)$$

In equations, h is the heat transfer coefficient, S is the surface area of the container, T_{max} is the equilibrium temperature and T_{surr} is the ambient temperature. A_{808} represents the absorption of FCO at 808 nm, and I was the incident laser power (1.8 W/cm^2). τ_s is time constant of the sample system, m_{H_2O} is the mass and C_{H_2O} is heat capacity of deionized water deionized water used as the solvent. The η value was 7.71% by calculating the experimental data.

5. The digital images of FCO-DOX dispersed in PBS and culture medium

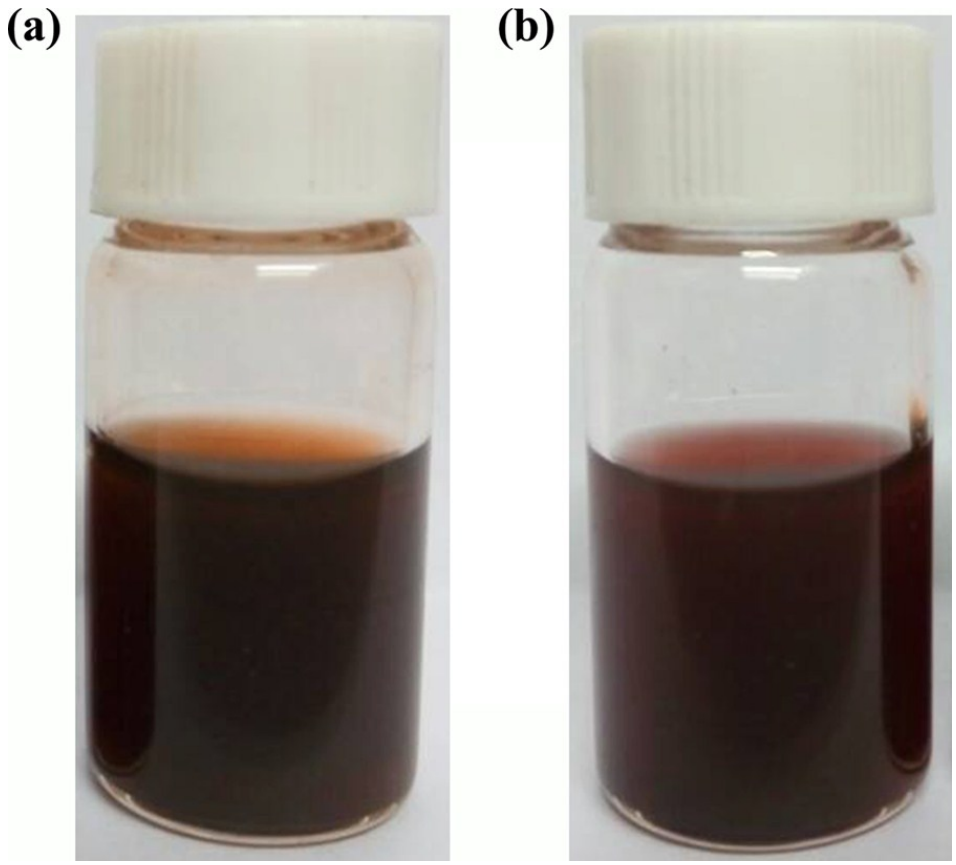

Fig. S5. The digital images of FCO-DOX dispersed in (a) PBS and (b) culture medium.

6. The drug release behavior

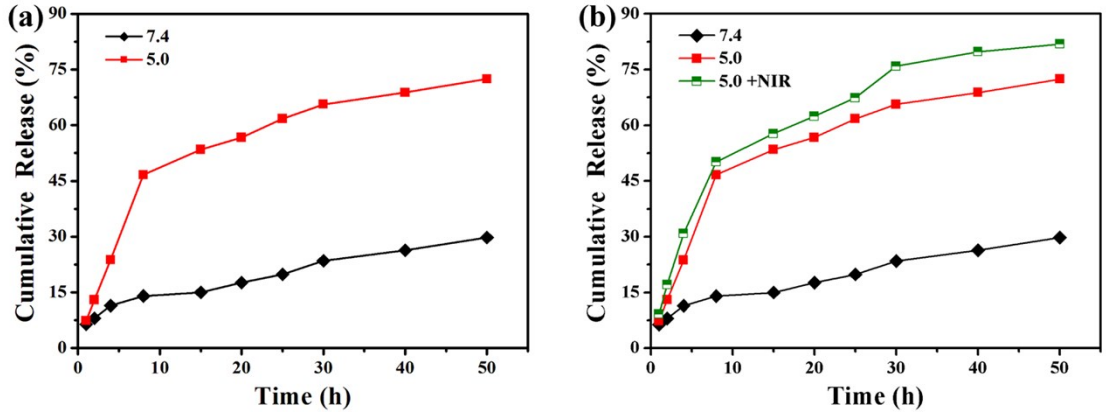

Fig. S6 (a) pH-responsive drug release of FCO-DOX. (b) NIR enhanced drug release.

7. The comparison of drug loading efficiency among different carriers

Drug carrier	Drug	Drug loading efficiency	Reference documentation
Sodium Alginate Conjugated Graphene Oxide	Doxorubicin Hydrochloride	183.4%	Int J Biol Macromol, 2016, 93, 582-590.
Porous Silicon Dioxide	Dexamethasone	5.96% -10.77%	Experimental Eye Research 129 (2014) 74-82
Zeolitic Imidazolate Framework-8 Coated Hollow Mesoporous Silica	Doxorubicin Hydrochloride	29.2%	J. Mater. Chem. B, 2017, 5, 2126--2132
Multiwalled Carbon Nanotube-Polyglycolic Acid	Doxorubicin Hydrochloride	152%	International Journal of Nanomedicine 2013:8 4427–4440
Poly (Trimethylene Carbonate)-B-Poly(L-Glutamic Acid）	Doxorubicin Hydrochloride	47%	Journal of Controlled Release 147 (2010) 428–435
Fluorinated Carbon Fiber Oxide	Doxorubicin Hydrochloride	84%	This work

8. The fluorescence intensity of the cellular uptake behavior with three parallel samples

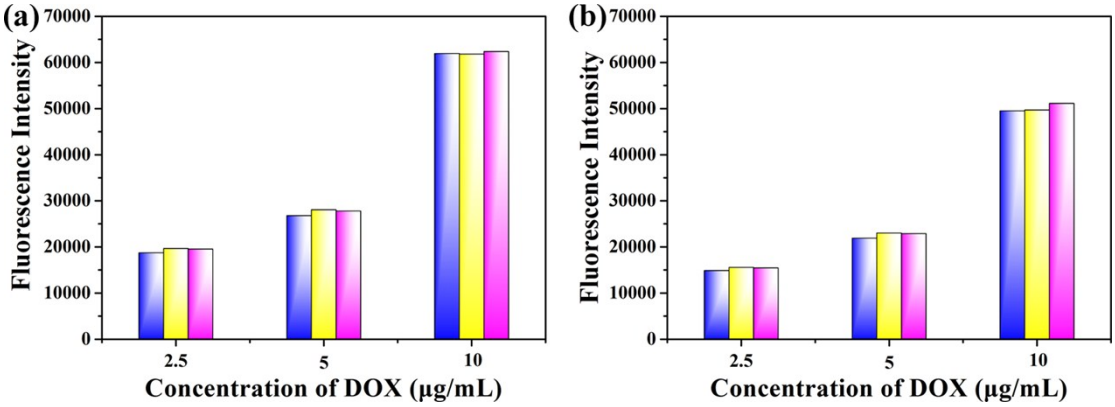

Fig. S8. The fluorescence intensity of (a) free DOX, (b) FCO-DOX obtained from three parallel samples

9. The viabilities of HeLa cells treated with free DOX with laser at 0.63 μg mL^{-1} and untreated cells with laser as FCO-DOX as control.

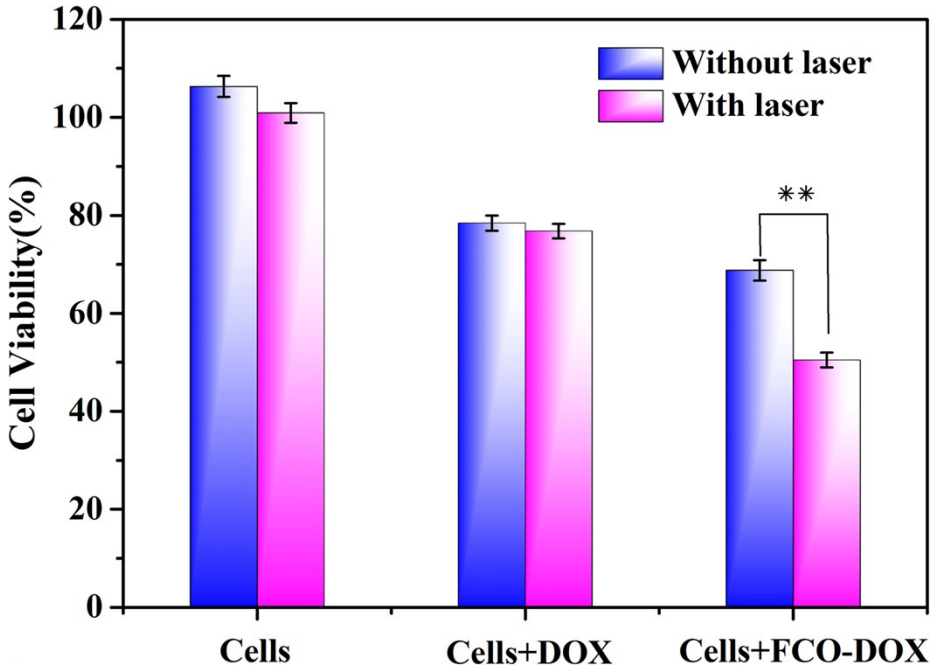

Fig. S9 The viabilities of HeLa cells with laser and cells incubated with free DOX at 0.63 μg mL^{-1} with laser, while FCO-DOX was used as the control.The ᴺᴺ indicated P<0.01.

Notes and References

1. D. K. Roper, W. Ahn and M. Hoepfner, *Journal of Physical Chemistry C*, 2007, **111**, 3636-3641.

2. X. Chen, M. Zhang, S. Li, L. Li, L. Zhang, T. Wang, M. Yu, Z. Mou and C. Wang, *Journal of Materials Chemistry B*, 2017, **5**, 1772-1778.

3 C. Sun, L. Wen, J. Zeng, Y. Wang, Q. Sun, L. Deng, C. Zhao and Z. Li, *Biomaterials*, 2016, 91, 81-89.

4 F. Mao, L. Wen, C. Sun, S. Zhang, G. Wang, J. Zeng, Y. Wang, J. Ma, M. Gao and Z. Li, *ACS Nano*, 2016, 10, 11145-11155.

5 L. Wen, L. Chen, S. Zheng, J. Zeng, G. Duan, Y. Wang, G. Wang, Z. Chai, Z. Li and M. Gao, *Advanced Materials*, 2016, 28, 5072-5079.